

Modeling of Thermal Behavior of Ancient Metallurgical Ceramics

Anno Hein[†] and Vassilis Kilikoglou

Institute of Materials Science, N.C.S.R. Demokritos, 15310 Athens, Greece

The finite element method is used to examine the thermal properties of functional ceramics, which were used in metallurgical processes during antiquity. Based on the ceramics' microstructure a model is developed considering the impact of porosity and inclusions and the heat transfer from ceramics to environment. An example of a Bronze Age copper smelting furnace from Cyprus is presented. Particularly the influence of pore shape and pore orientation on the thermal conductivity is investigated. Temperature development in the entire furnace is simulated and compared with estimations of the firing temperature in particular areas of the furnace.

I. Introduction

IN the history of humankind and material culture the utilization and processing of metals marked an important step. The initial exploitation and processing of pure metals was soon followed by the utilization of metal ores, which required the development of elaborate metallurgical techniques. These included, apart from generation of necessary process temperatures and use of suitable fluxes, the production of heat resistant tools, such as furnaces, tuyères, moulds, or crucibles. The main material used for the production of these equipment was ceramic, a material with a long history of production and with beneficial properties in terms of refractoriness and heat insulation. Common pottery clays, in antiquity, were usually fired at temperatures up to 1100°C, as they would normally distort at higher temperatures. This behavior was due to the nature of the raw materials, comprising considerable amounts of basic components such as CaO, MgO, K₂O or Na₂O, which were reacting at comparatively low temperatures.¹ Furthermore, the raw materials contained natural inclusions in the clay matrix, most commonly quartz, feldspars, micas, but also other kinds of minerals and rock fragments, depending on the particular geological environment. Therefore, for the production of metallurgical ceramics either more refractory clays had to be selected or the clay paste preparation and ceramic construction had to be modified, in order to enable them to withstand high temperatures.

A variety of approaches to improve the thermal properties of archaeological ceramics, used at high temperatures, have been reported in the bibliography. A common approach was the fabrication of rather thick walls, which stabilized the ceramic body and reduced heat transfer. In this way, thermal stresses were suppressed due to smaller temperature gradients. Another common technique was the generation of porosity, either by adding organic material to the unfired clay body, which was burned out during firing, or by the ways clay was processed and wedged. Apart from reducing heat transfer, pores and voids improved the toughness of the ceramic body by interrupting the propagation of cracks in the matrix.² Finally, high volume fractions of non-plastic inclusions were added to improve the refractory properties of the ceramic body. Thermally inert inclusions, such as

quartz, stabilized the ceramic matrix at temperatures at which clay minerals started to decompose. Furthermore, due to heat expansion coefficients, different from the ceramic matrix, inclusions generated microcracks and therefore additional porosity.

Apart from sufficient refractoriness, depending on the type of heat source and the direction of the heat, different material properties of the ceramics are required concerning heat insulation and thermal shock resistance. For example, internal heating, like in a smelting furnace, requires low thermal conductivity in order to maintain the heat. On the contrary, when the heating source is external, like in a crucible, high thermal conductivity is required to accelerate heating of the content. At the same time moulds should exhibit high resistance to thermal shock. Furthermore, mechanical properties, such as strength and toughness, had to be regarded as they are both related to thermal performance.

A technological investigation of metallurgical ceramics from a Bronze Age copper smelting site in Cyprus, conducted by the authors,³ revealed that a considerable improvement in the refractoriness was achieved by the addition of volcanic temper and sand, and at the same time increased porosity ensured thermal insulation of the furnaces. It also became apparent that modeling of heat transfer in ceramics was necessary in order to interpret analytical results. The present article focuses on two aspects of the modeling. First, thermal properties of archaeological ceramics will be assessed in relation to their microstructure (shape of inclusions and porosity). Secondly, an example of macroscopic modeling will be presented, demonstrating examination of ceramic function and metallurgical process. Using reconstructed size and shape of the smelting furnaces, parameters like temperature and length of the smelting process and environment of the furnaces were investigated. The results were compared with temperature profiles in furnace fragments, which were estimated by observations of the microstructure under the scanning electron microscope (SEM).

II. Archaeological Evidence

The technological aspects modeled in this paper are based on evidence coming from the detailed study of metallurgical ceramics from Cyprus, previously conducted by the authors,³ as well as on work published in the bibliography.^{4–10}

(1) Metallurgical Ceramics from Politiko-Phorades (Cyprus)

Politiko-Phorades is the earliest primary copper smelting site discovered in Cyprus up to now, dated approximately 1600 BC, which is the beginning of the Late Bronze Age. It is located in the northeast foothills of the Troodos Mountains, probably as one of a chain of similar sites close to the mines where the copper sulfide ores were exploited. Politiko-Phorades represents the start of a period of large-scale copper production in Cyprus, acting as a supplier of Eastern Aegean and other regions of the Mediterranean.^{11,12} Apart from slag remains, a large number of ceramic fragments was discovered, which provided basic information about the construction of furnaces and tuyères and their use.

Out of the ceramic assemblage, 15 tuyère fragments and 25 furnace fragments were selected for more detailed examination.³

D. Green—contributing editor

Manuscript No. 22049. Received July 24, 2006; approved October 26, 2006.

[†]Author to whom correspondence should be addressed. e-mail: hein@ims.demokritos.gr

According to analytical results, the raw materials used for fabrication of the metallurgical ceramics were local non-calcareous clays, similar to the illitic clays used in contemporary pottery production, albeit comparatively coarse. Their microstructure was dominated by inclusions of volcanic rock fragments, apparently related to the local geological environment. Porosity was intentionally generated in the ceramic body, as indicated by the clear traces of burned out organic fibres. Other frequent and elongated voids were apparently related to processing of the coarse clay paste without extensive mixing or compressing.⁴ Open porosity was found to be around 25% for a typical tuyère and up to almost 40% for some furnace wall fragments. In all samples, a preferred orientation of pores and voids parallel to the surface was noticed, apparently generated during construction. Finally, furnaces and tuyères presented no significant difference in terms of raw materials and fabrication technique, although the furnace fragments generally appeared to present higher proportions of coarse inclusions. The furnaces had cylindrical shape with an outer diameter of 420–440 mm and they were made entirely of clay. They presented a thick base of 40–50 mm and walls of 30–40 mm with well-defined rims. Occasional finger impressions on the outside of the furnace walls indicated freestanding construction of the furnaces. Therefore, in the modeling that follows the possibility had to be considered that at least a part of the furnace outside was exposed to air during use.

(2) Further Case Studies

Former studies on ancient metallurgical furnaces concerned primarily furnace linings, but also crucibles and moulds were examined.^{4–10} The studies revealed a variety of methods in order to improve the thermal performance of the material. In most cases this was achieved by non-plastic inclusions, either intentionally added as temper to the clay paste or a natural ingredient. Quartz was determined in most cases, but also slag remains,¹⁰ grog or carbonaceous materials, such as charcoal or graphite. Carbonaceous materials additionally were assumed to inhibit the oxidation of the molten metal.⁹ The widespread and systematic use of kaolinitic clays, i.e., fireclays, became common only since the Roman period.⁹ In many cases tempering with organic materials was observed, though the related high porosity was not generally assumed as an advantage, especially in view of the vessel strength. The addition of organic temper, particularly fibrous materials, was usually assessed as advantageous for strengthening the unfired ceramic body and as a carbon source.⁹

In some studies of furnace linings, the heat transfer during use also was considered and the operation time was estimated by observation of the degree of vitrification in the ceramics in different distances from the furnace inside.^{5,8,10}

III. Heat Transfer in Ceramics

For estimations about the temperature developments in particular parts of the furnaces and about their operation conditions, the heat transfer during the smelting process has to be examined. Therefore, primarily two heat transfer processes have to be considered, heat conduction and heat convection. In the present model, heat transfer by radiation will be neglected because it is expected to be small at the assumed temperatures.¹³

Heat conduction depends on the thermal conductivity k of the specific material which describes the heat flux dQ/dt normal to an area A under a particular temperature gradient ∇T .¹⁴ Typical values for thermal conductivity of ceramics are in the range of 0.5–1.5 $W \cdot (m \cdot K)^{-1}$, normally with decreasing values for higher temperatures. For a single crystal, however, possible anisotropy of the thermal conductivity has to be considered.¹⁴ Particularly phyllosilicate minerals, due to their platy crystal structure, present a lower thermal conductivity perpendicular to their main orientation. As long as crystals are randomly oriented in the material the effective thermal conductivity arises from the mean thermal conductivity. But in the case of a preferred orien-

tation of the phyllosilicate minerals, anisotropy of the thermal conductivity also could emerge macroscopically.

In the case that the temperature in the material is not constant, the temperature development depends on the thermal diffusivity α , which is the ratio of the thermal conductivity k and the heat capacity per unit volume $\rho \cdot c_p$, where ρ is the density of the material and c_p is the heat capacity. For ceramics α is typically in the range of 0.5–1.0 mm^2/s . The temperature change is described by a partial differential equation, the heat conduction equation:¹⁴

$$\frac{\partial T}{\partial t} = \alpha \cdot \nabla^2 T \quad (1)$$

The second heat transfer process to be considered is heat convection, being heat transfer between a solid surface and a moving fluid with different temperature, in the present case the air outside the ceramics. The film coefficient of the fluid describes the heat flux through an area A of the solid's surface subject to the temperature difference between surface temperature T_s and the bulk temperature of the fluid T_∞ . In earlier studies of archaeological furnace linings, estimations of heat transfer were focussed on heat conduction only, using an analytical solution of the heat conduction equation (Eq. (1)) and assuming infinitely thick ceramic layers.^{5,8,10} But in the case of a furnace wall with finite thickness, the outer surface of which is exposed to air, heat convection at the ceramic/air interface has to be considered. The film coefficient for air is in the range of 10–100 $W \cdot (m^2 \cdot K)^{-1}$ depending on humidity and the velocity of the air draft, i.e., the wind force at the ceramic surfaces.

Developing a model of an entire smelting furnace, different cases of heat transfer from furnace into environment will have to be distinguished. In all cases it will be assumed that the inner surface of the ceramics was in direct contact with the smelting load, which acted as heat source. At a first stage, the parameters which affect the heat transfer, such as microstructure and porosity, are modeled in order to understand their impact on the manufacturing technology and then the procedure for modeling of the operation of the entire furnace is described.

IV. Model

(1) Microstructure: Multiphase Composite

Archaeological ceramics were complex composites, consisting of the actual ceramic matrix, commonly a mixture of different clay minerals and respective high temperature phases, of pores and voids with various shapes and dimensions and of miscellaneous non-plastic inclusions, such as quartz, feldspars, carbonates, micas, or rock fragments. Therefore, regarding thermal properties, the microstructure of archaeological ceramics can be described as a multiphase composite. As the main component, the actual ceramic matrix forms a more-or-less continuous phase. Pores and voids, with clearly lower heat capacity and conductivity, act as heat barriers and form the second phase. Finally, the non-plastic inclusions form further phase, of considerable volume fraction. These inclusions commonly present higher densities than the ceramic matrix and different thermal properties.

The effective heat capacity c_{eff} of the composite can be expressed as:

$$c_{\text{eff}} = \sum_i v_i \cdot c_i \quad (2)$$

with c_i the heat capacities of the particular phases and v_i their particular volume fractions. In the same way the effective density ρ_{eff} can be determined.

The effective heat conductivity k_{eff} is more complex because it depends on the geometrical arrangement of the phases.¹⁴ The simplest geometry is to consider parallel layers of the different materials. Although this arrangement is commonly not observed, it is of interest because it provides upper and lower limits for a particular multiphase composition. The upper limit of

conductivity corresponds to heat flow parallel to the layers' orientation and can be calculated in the same way as k_{eff} and ρ_{eff} . The lower limit for k_{eff} corresponds to a heat flow perpendicular to the layers' orientation and it is given by:

$$\frac{1}{k_{\text{eff}}} = \sum_i \frac{v_i}{k_i} \quad (3)$$

There are more appropriate models, such as the Maxwell model describing isolated pores with thermal conductivity of k_{por} , dispersed in a solid phase with thermal conductivity of k_{solid} .^{13–15}

$$\frac{k_{\text{eff}}}{k_{\text{solid}}} = \frac{2 + \kappa + 2 \cdot \Pi \cdot (\kappa - 1)}{2 + \kappa - \Pi \cdot (\kappa - 1)} \quad (4)$$

where Π is the porosity and $\kappa = k_{\text{por}}/k_{\text{solid}}$. This model, however, is rather suitable for dense ceramics with $\Pi < 20\%$. As for the whole range of porosity in a continuous solid phase a more general interpolation formula can be used:¹³

$$\frac{k_{\text{eff}}}{k_{\text{solid}}} = (1 - \Pi)^{3/2} + \Pi^{1/4} \cdot \frac{k_{\text{por}}}{k_{\text{solid}}} \quad (5)$$

where k_{solid} is the effective thermal conductivity of the solid part of the composite.

According to these considerations, in the extreme case of 40% porosity, the conductivity of the solid phase would be reduced to approximately 50%. This would concern, however, arbitrarily dispersed and shaped pores. But the observed ceramic microstructure with elongated pores oriented perpendicular to the heat flow would be expected to have a stronger reducing effect on the heat transfer.

(2) Two-Dimensional Models

In reality, the calculation of k is not straightforward, especially when preferred orientation of the phases exists.¹⁶ Therefore, numerical solution using finite element method (FEM) was chosen in order to assess the effect of certain microstructure arrangement. To generate realistic two-dimensional models of multiphase microstructures, element maps of polished surfaces obtained by SEM were evaluated with image processing. In Fig. 1 an example SEM micrograph is presented with the corresponding three-phase model, considering ceramic matrix, pores, and quartz inclusions. In this example the pixel size and hence limit for the size of quartz inclusions or voids was approximately 2.6 μm .

In order to examine the thermal conductivity of a particular region in the sample by FEM, an area representing this region

was created and meshed with PLANE77 elements. Each element corresponded to a pixel of the region and according to the multiphase model the respective material properties were attributed to each of the elements. For the thermal conductivity, the following values were assumed: $k_{\text{ceramics}} = 1.0 \text{ W} \cdot (\text{m} \cdot \text{K})^{-1}$, $k_{\text{air}} = 0.024 \text{ W} \cdot (\text{m} \cdot \text{K})^{-1}$ and $k_{\text{quartz}} = 1.8 \text{ W} \cdot (\text{m} \cdot \text{K})^{-1}$. A temperature gradient was simulated by applying different temperatures on two opposite sides of the model area (i.e., the internal and external surfaces of the ceramic body). The FEM solution of the described system provided the temperature distribution in the area and the heat flux in every element. Finally, the effective thermal conductivity could be estimated by evaluating the average heat flux. In Fig. 2(a) an example 150 \times 150-pixel area is presented, which corresponds to a section from the model in Fig. 1. A temperature difference of 100 K was applied between the top side and the bottom side of the model area, assumedly parallel to the actual heat flux during furnace operation. Figure 2(b) presents the resulting heat flux in direction of the applied heat gradient. In this case the average heat flux was lower than in a similar area built entirely of elements with the assumed material properties of the clay matrix. This observation indicates the strongly reducing effect of the voids on the thermal conductivity.

A series of six SEM micrographs of one tuyère and two furnace sections, with porosities between 5% and 50%, was then evaluated in order to examine particularly the effect of porosity. From the above-described example it became clear that the effect of the quartz inclusions on the thermal conductivity was small compared with the one of porosity. Therefore, quartz was not considered as an independent phase and the problem was reduced to a two-phase model, representing the solid part, i.e., clay matrix with inclusions, and voids. Regarding Fig. 2, 150 \times 150-pixel model areas were selected and evaluated simulating a temperature gradient in the assumed direction of the actual heat flux and for comparison in a 90° rotated direction. The relative effective thermal conductivity of the ceramic/void compound was compared with theoretical values according to Eq. (5). The results indicated clearly an additional reduction of the thermal conductivity compared with the case of spherical and arbitrarily distributed pores, from approximately 10% for the smallest porosity values up to almost 70% for the highest determined porosity (Fig. 3). Furthermore, except for a few model areas, which included one large unusually oriented pore, the reduction was particularly extreme in direction of the assumed heat flux. Also the influence of the pore orientation appeared to be larger for higher porosities, from 5% up to a factor 2. Hence the observed microstructure, which was assumedly intentionally created by the ancient craftspeople by the specific forming process and the addition of organic temper, enhanced the heat insulation of the metallurgical ceramics (furnaces and

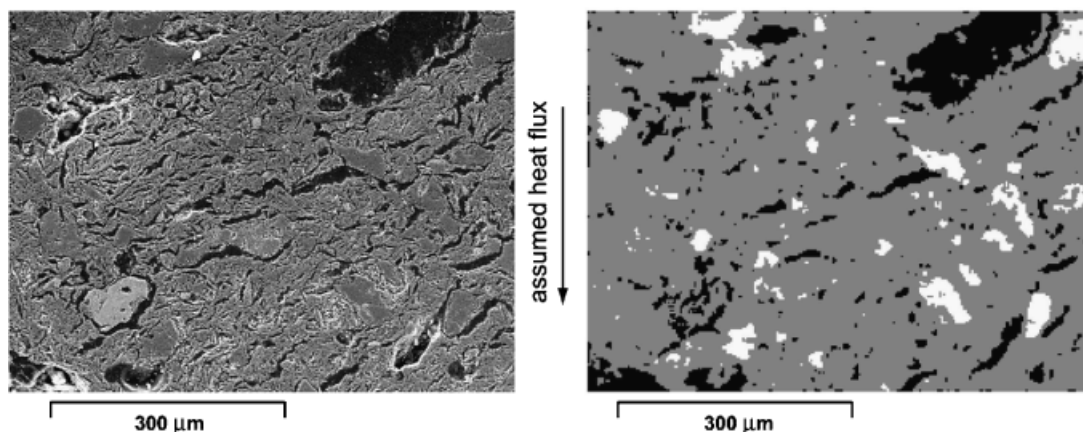


Fig. 1. (a) Scanning electron microscope (SEM) picture of a polished surface sample from a tuyère from Politiko-Phorades: the heat supposedly was flowing from the top to the bottom. (b) Three-phase model of the sample according to an Si element map of the section presented in the SEM picture: gray, ceramic matrix; black, void; white, quartz inclusion. The pixel size corresponds to c. 2.6 μm .

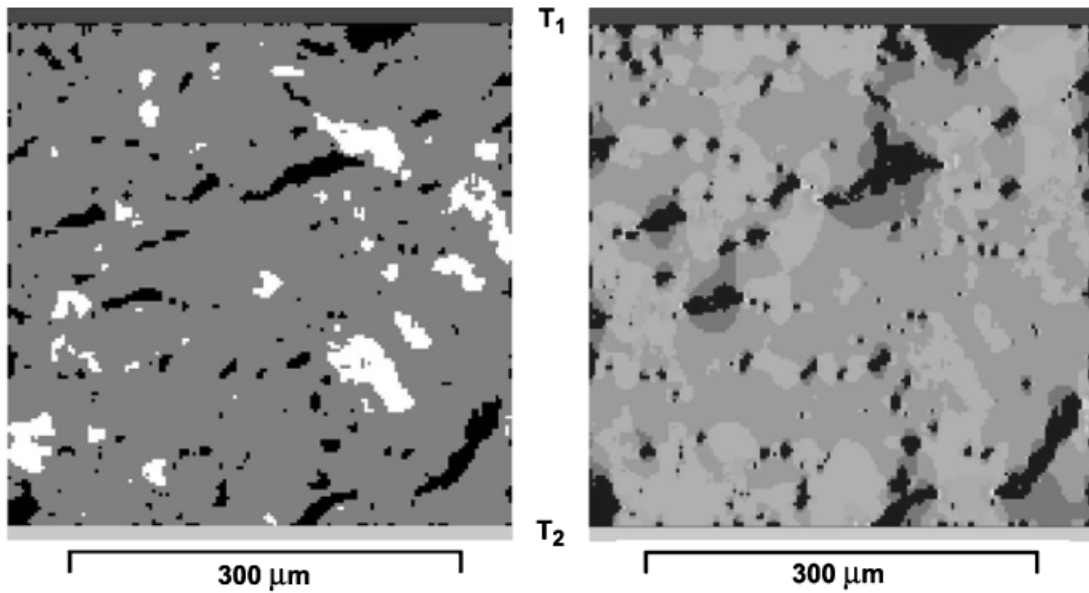


Fig. 2. (a) Subsection of the three-phase model presented in Fig. 1(b): the subsection corresponds to a 150×150 element area, with each element attributed with the particular material properties. For the finite element method (FEM) evaluation a temperature gradient is simulated from top to bottom. (b) Heat flux in each element as calculated by FEM: regions of low heat flux (dark) correspond to the areas of the pores whereas the regions of high heat flux (light) correspond to quartz grains and narrow spaces between the pores.

tuyères). It has already been shown that Bronze Age technological parameters, such as orientation of inclusions, were controlled during pottery formation.¹⁷

In order to evaluate the role of shape and orientation of the pores, ellipses were fitted to the voids. Image processing provides information about ratio of minor to major axes and orientation of ellipses, which are representing the voids as approximation.¹⁸ In this way a series of sections of tuyère and furnace fragments was examined using the public domain image processing software *ImageJ* for particle size analysis of the corresponding Si element maps. Figure 4 presents an ellipse fit in a tuyère section, representing the same area as the one of Fig. 1. Sizes, shapes, and orientations of the ellipses in this area and three other areas in the same section are presented in Fig. 5. It can be seen that there is a concentration of points toward the left part of the plot. Figure 6 indicates an orientation of the voids with angles of 0° – 30° of the minor axes to the assumed heat flux. Furthermore, the majority of the fitted ellipses showed ratios of

minor to major axes below 0.5. The main outcome is that there is preference for elongated voids which are placed almost perpendicular to the actual heat flux. The observed trend appeared to be clearer in the case of larger voids.

(3) Three-Dimensional Models

It has to be considered that two-dimensional models of the material's microstructure describe the heat transfer only insufficiently, because one degree of freedom is neglected. It has been shown, however, that a two-dimensional model provides a lower limit for the thermal conductivity and for this reason it is useful in the modeling practice.¹⁹

The development of realistic three-dimensional models based on the above-presented examination of two-dimensional sections is not straightforward. Considering three dimensions the effect of pore shape and orientation can be examined by assuming spheroid shaped voids. In this case Eq. (5) can be generalized by introducing an additional shape factor and preferred orientation.¹⁶ Alternatively, unit cells models can be examined, with a single spheroid shaped pore of particular shape and orientation.

A possible approximation of a three-dimensional void structure can be modeled with randomly distributed spheroid shaped voids.²⁰ Typical shapes and orientations of the spheroids are provided by the above described ellipse fit. However, by using

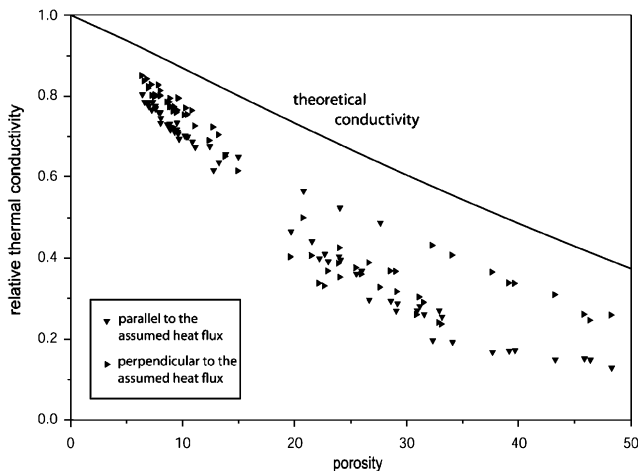


Fig. 3. Relative effective thermal conductivity in model areas with different porosity: presented are simulated thermal conductivities in direction of the assumed heat flux and for comparison in a 90° rotated direction. The curve presents the theoretical conductivity correlated with porosity according to Eq. (5).

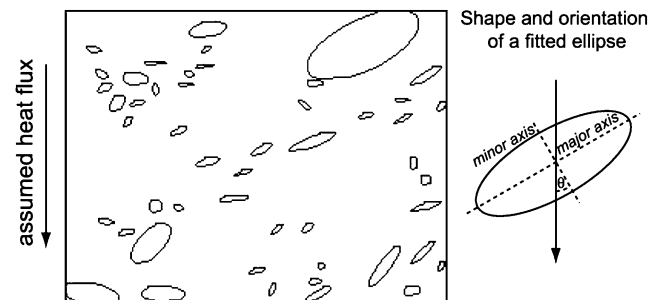


Fig. 4. Ellipse fit of the voids in the micrograph presented in Fig. 1 according to the Si element map of the section: the minimum size of the fitted ellipses was 20 pixels corresponding to $135 \mu\text{m}^2$. The porosity according to the ellipse fit was 11.2%.

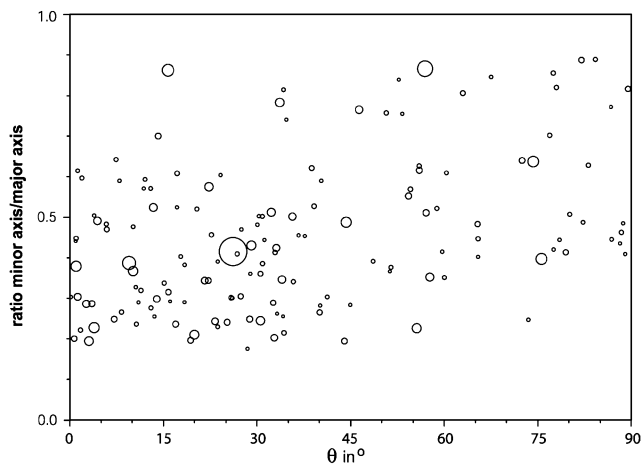


Fig. 5. Ratio of minor axis to major axis of fitted ellipses against the angle of the major axis to the assumed heat flux: the ellipses correspond to the voids of different areas in the sample presented in Fig. 4. The size of the symbols corresponds to the relative size of the ellipses, the whole range of which is presented in Fig. 4.

only spheroid shaped voids, the actual void structure might be described incompletely. In the case study presented, for example, some of the voids had an irregular shape, originating from burned organic fibers. Therefore, a complete three-dimensional model, considering different types of void shapes, is planned to be developed in a future study.

(4) Additional Effects

Apart from the interference by the spatial distribution of pores and inclusions, there are other processes which influence the effective heat conduction in the metallurgical ceramics.^{13,21} For example, in the case of extended pores or cracks, heat convection within the pores can play a role in heat transfer. Furthermore, thermal radiation emerges, which, however, reaches considerable intensities only at temperatures above 1200°C. Whereas the ceramic matrix itself is relatively transparent for the respective wavelengths (at 1200°C) thermal radiation affects the heat transfer in large pores.¹³

Finally, when ceramics are heated, voids may be reduced in size due to sintering and cracks may close by relaxation of thermal mismatch stresses. Therefore in these cases the thermal conductivity increases with increasing temperature. Additionally, in the case of unfired or low-fired ceramics, the microstructure changes completely when temperatures are reached at which the

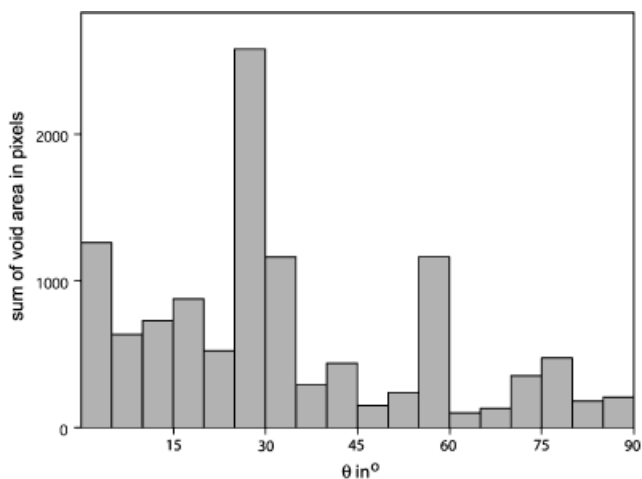


Fig. 6. According to Fig. 5, the sum of the void areas in pixels are presented against certain ranges of the angle of the major axis to the assumed heat flux.

clay minerals start to decompose and the matrix vitrifies. Apart from general change in microstructure the heat transfer is also affected by the energy consumed by phase transformation.

(5) Two-Dimensional Model of a Smelting Furnace

Based on archaeological evidence from ceramics excavated in Politiko-Phorades and the considerations from the basic calculations of the previous section, a furnace model was designed to answer questions about its function and smelting process. Furnace size and shape, reconstructed from excavated fragments, were used to compile a two-dimensional model for evaluation with finite element analysis (Fig. 7). The thermal properties, which were applied to the ceramic body, were based on the considerations about the microstructure and porosity, described in detail in the previous paragraphs. Therefore, for the ceramics a thermal conductivity of $0.4\text{--}0.6\text{ W}\cdot(\text{m}\cdot\text{K})^{-1}$ was assumed with values increasing with the temperature. This would correspond to ceramics with porosity of approximately 35%–40% and a thermal conductivity of $1.0\text{ W}\cdot(\text{m}\cdot\text{K})^{-1}$ of the actual ceramic matrix. The density of the ceramics was assumed with $1500\text{ kg}/\text{m}^3$ and its specific heat capacity with $900\text{ J}\cdot(\text{kg}\cdot\text{K})^{-1}$. The temperature $T_{\text{in}}(x, y, t)$ applied as load on the inner furnace surface was correlated with the assumed necessary temperature of the smelting process. Based on temperature estimations in polished sections in different distances from the surface, the peak temperature at the exposed inner surface was estimated approximately between 1150° and 1200°C³ (Fig. 8). Therefore in the particular areas the degree of vitrification was determined by SEM and compared with samples, which were refired at controlled temperatures under oxidizing and reducing conditions. Presuming a sufficiently homogeneous matrix the temperature gradient was assumed as linear. The heating period until reach-

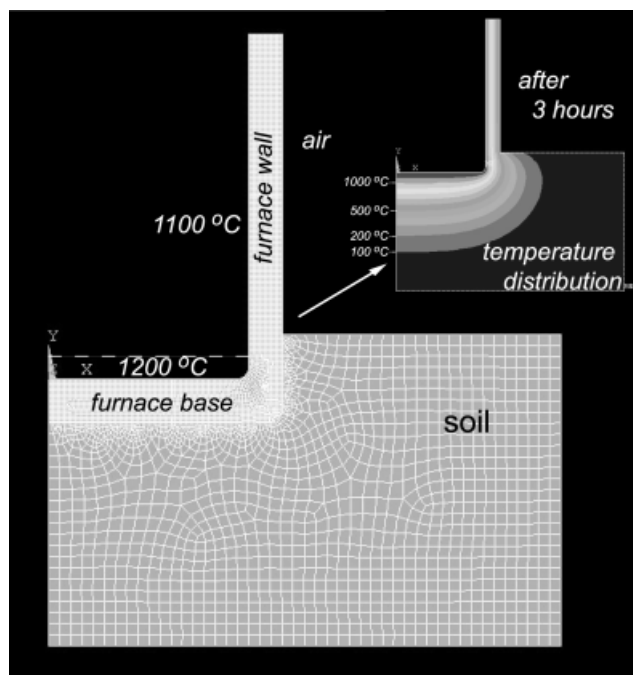


Fig. 7. Two-dimensional finite element method model of a copper smelting furnace: the model corresponds to a cut through a cylindrical furnace from the center to the wall. The furnace was assumed to be buried up to a certain height into the soil. Parts of the furnace wall and the surface of the soil were assumed to be exposed to the air simulating heat convection. Furnace and soil were meshed with PLANE77 elements. A heat source of 1200°C was simulated for the lowest part of the furnace inside and a temperature of 1100°C for the inner surface of the furnace wall. In the upper right part the temperature distribution after 3 h is presented. The temperatures in different distances from the heat source are indicated by color variation using a step width of 100°C. Certain temperatures are additionally specified following the section through the furnace center.

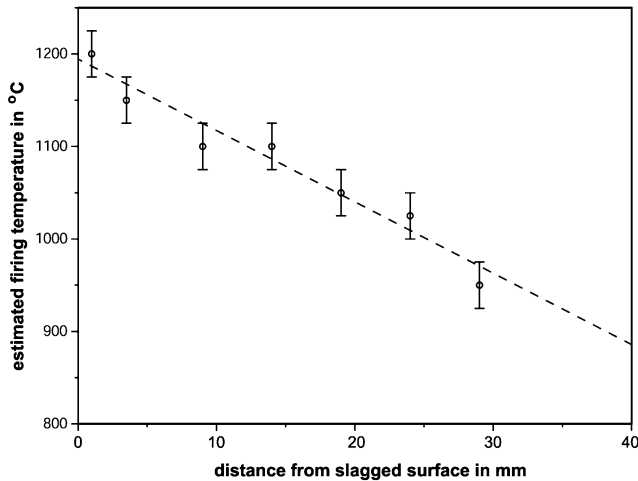


Fig. 8. Temperature gradient in a furnace base fragment from Politiko-Phorades based on scanning electron microscope observations: assuming stable conditions and a sufficiently homogeneous ceramic matrix, a linear slope was fitted to the temperature estimations.

ing the peak temperature remained unknown but it was assumed as short compared with the operation time. Another unknown set of constraints concerned the environment of the furnace. The furnace base was in contact with soil, the thermal properties of which could be only roughly estimated. Furthermore, there was the possibility that the furnace was buried up to a certain level into the soil or standing against a stone wall. In all these cases the heat transfer from furnace wall to soil or stone had to be considered. Alternatively, a freestanding furnace wall could be assumed or a furnace wall, which was exposed at least in part to air—most possible, in view of the final tapping of the furnace to extract the metal. As for the outer surface of the furnace, for the part that it was exposed to air, heat convection had to be considered, which depended on the air temperature and, more important, on the wind speed. For the present simulation a film coefficient of $30 \text{ W} \cdot (\text{m}^2 \cdot \text{K})^{-1}$ with an ambient temperature of 25°C was assumed, corresponding to a moderate wind speed. As for the soil the thermal conductivity was assumed with $1.0 \text{ W} \cdot (\text{m} \cdot \text{K})^{-1}$, its density with 2500 kg/m^3 , and its specific heat capacity with $900 \text{ J} \cdot (\text{kg} \cdot \text{K})^{-1}$. The parameters were evaluated with transient FEM analysis of the model. In this way the temperature development in particular areas of the furnace could be examined (Figs. 9 and 10). Furthermore, the comparison of the simulated temperature development with the temperature estimations based on SEM observations (Fig. 8) was expected to provide information about the operation time of the furnace.

The simulation showed that the temperature gradient in a freestanding furnace wall with a thickness of 30 mm would come to equilibrium after approximately 30 min (Fig. 9). The temperature at the outer surface depended on the thermal conductivity of the ceramics and on the film coefficient of the air, which was related to the assumed wind force.²² This result corresponded to the SEM observations of furnace wall fragments, which showed only a small layer of vitrified ceramics at the inner surface and a steep temperature gradient to the outer surface.³ On the other hand, the simulation indicated that ceramic walls, which were in contact with air during a metallurgical process, are scarcely applicable to estimate the operation time, because, as it was shown, the time period in which the temperatures in the walls reached stable conditions, was comparably short. Therefore the observed degree of vitrification could lead to underestimation of the operation time.

In contrast to the furnace walls, the furnace base fragments presented thicker layers of vitrified ceramics and smaller temperature gradients. This corresponded to the FEM simulation concerning the furnace parts, which were in contact with the soil. Here, the heat was conducted from the furnace into the soil over the entire operation period with a continuing temperature increase in the ceramics (Fig. 10). Even though the temperature

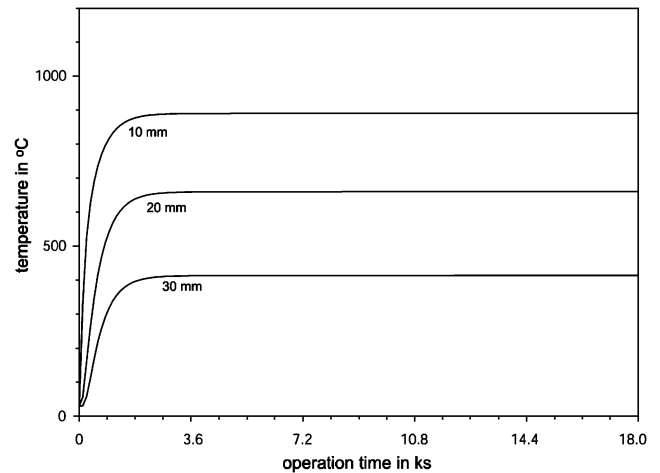


Fig. 9. Simulated temperature development in the furnace wall in different distances from the inner surface. The examined part of the wall was assumed to be exposed to air at the outside surface. An operation time of 5 h was simulated. The temperatures in this simulation, however, reach equilibrium after approximately 30 min.

increase was slowing down, a clear correlation between temperatures in certain distances from the inner surface and operation time could be confirmed in the simulation. This correlation could be used to estimate the operation time of a typical furnace with approximately 4 h under the assumed conditions. In order to assess the possible error for this estimation, further simulations were conducted assuming temperature independent thermal conductivities of 0.8 , 0.6 , and $0.4 \text{ W} \cdot (\text{m} \cdot \text{K})^{-1}$. The respective estimated operation time was between 3 and 6 h. Apart from the thermal conductivity of the furnace, the thermal conductivity of the soil also affected the temperature development in the furnace base. Therefore, for more accurate simulation of temperature development in the furnace, the environment and possible furnace location has to be examined. Furthermore, laboratory measurements of thermal properties of the ceramics will complement the theoretical considerations based on the observed microstructure. Finally, apart from the simulation of the temperature development, the furnace model also allows for an assessment of the thermal stress in the ceramic body, considering thermal expansion and fracture strength of the ceramics.

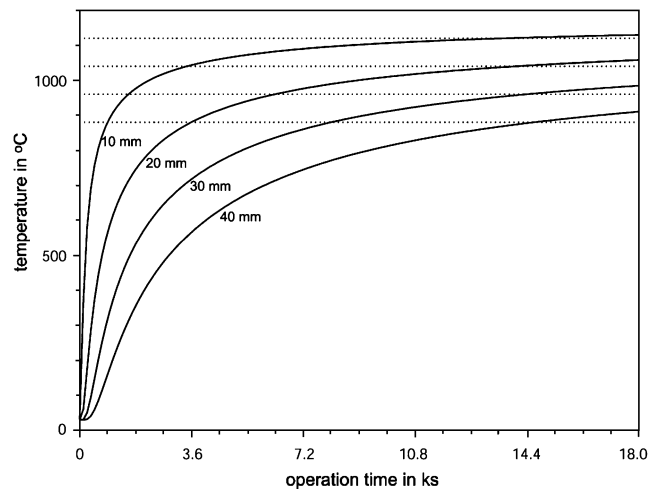


Fig. 10. Simulated temperature development in the furnace base in different distances from the inner surface. An operation time of 5 h was simulated. The dotted lines correspond to the assumed peak temperatures for the particular distances in the presented case study, based on the estimations presented in Fig. 8. In this simulation the respective temperatures are reached after approximately 4 h.

V. Conclusions

The multiphase model of the ceramic matrix presented here provided an assessment of the thermal properties of ancient metallurgical ceramics on the basis of their microstructure, considering the distribution of pores and non-plastic inclusions in their ceramic matrix. In this way particular methods of ceramic construction, which were used in antiquity to create materials with sufficient thermal properties, can be investigated with the FEM. In the specific case of fragments of Bronze Age copper smelting furnaces from Cyprus, the study demonstrated the beneficial effect of porosity and particularly the orientation of the pores on the reduction of thermal conductivity. Non-plastic inclusions influenced the heat transfer rather indirectly by generating additional porosity and fulfilled otherwise a function in strengthening the ceramic matrix.

In the second part of the presented study a model of an entire furnace was presented and an attempt to reconstruct the temperature development in an ancient furnace during its operation. Temperatures in actual furnace fragments were estimated by the observation of the degree of vitrification with SEM. In this way parameters, such as process temperature and operation time, could be examined. It was found that in the areas of the furnace which were exposed to air, equilibrium could be reached approximately in 30 min and for this reason operation time cannot be extracted from the study of these ceramic parts. On the other hand, modeling of the ceramic parts which were in contact with the soil, an operation time of 3 h could be estimated. Apart from providing realistic estimations of these parameters, the simulation indicated the dependence on further parameters such as the heat convection in the surrounding air or the position of the furnace.

Studies like the present help to understand how ancient craftspeople constructed technical ceramics that could be used in high temperature processes. Furthermore, the ceramic remains provide valuable indications for details of the actual metallurgical process.

Acknowledgments

The authors would like to thank V. Kassianidou, who provided the investigated metallurgical ceramics and helped with discussions over the operation of the furnaces, and M. Catapotis and Y. Bassiakos, who gave them the opportunity to participate in a smelting experiment with a reconstructed perforated shaft furnace.

References

- ¹W. Noll, *Alte Keramiken und ihre Pigmente*. E. Schweizerbart'sche Verlagsbuchhandlung, Stuttgart, 1991.
- ²V. Kilikoglou, G. Vekinis, Y. Maniatis, and P. M. Day, "Mechanical Performance of Quartz-Tempered Ceramics: Part I, Strength and Toughness," *Archaeometry*, **40** [2] 261–79 (1998).

³A. Hein, V. Kilikoglou, and V. Kassianidou, "Chemical and Mineralogical Examination of Metallurgical Ceramics from a Late Bronze Age Copper Smelting Site in Cyprus," *J. Arch. Sci.*, **34**, 141–54 (2007).

⁴J. Baylay, I. C. Freestone, A. Jenner, and A. Vince, "Metallurgy," *London and Middlesex Archaeol. Soc. Spec. Paper*, **12**, 398–405 (1991).

⁵W. D. Kingery and W. H. Gourdin, "Examination of Furnace Linings from Rothenberg Site #590 in Wadi Zaghra," *J. Field Archaeol.*, **3**, 351–3 (1976).

⁶R. F. Tylecote, "Metallurgical Crucibles and Crucible Slags"; pp. 231–43 in *Archaeological Ceramics*, Edited by J. S. Olin and A. D. Franklin. Smithsonian Institution Press, Washington, 1982.

⁷G. Schneider and G. Zimmer, "Technische Keramik aus antiken Bronze- und Eisenwerkstätten in Olympia und Athen," *Berliner Beiträge zur Archäometrie*, **9**, 17–60 (1984).

⁸M. S. Tite, I. C. Freestone, N. D. Meeks, and P. T. Craddock, "The Examination of Refractory Ceramics from Metal-Production and Metalworking Sites"; pp. 50–5 in *The Archaeologist and the Laboratory, CBA Research Report 58*, Edited by P. Phillips. Council for British Archaeology, London, 1985.

⁹I. C. Freestone, "Refractory Materials and Their Procurement"; pp. 155–62 in *Archaeometallurgie der Alten Welt—Old World Archaeometallurgy, Der Anschnitt Beiheft 7*, Edited by A. Hauptmann, E. Pernicka, and G. A. Wagner. Deutsches Bergbau-Museum, Bochum, 1989.

¹⁰M. S. Tite, M. J. Hughes, I. C. Freestone, N. D. Meeks, and M. Bimson, "Technological Characterisation of Refractory Ceramics from Timna"; pp. 158–75 in *The Ancient Metallurgy of Copper*, Edited by B. Rothenberg. Institute for Archaeometallurgical Studies, London, 1990.

¹¹A. B. Knapp, M. Donnell, and V. Kassianidou, "Excavations at Politiko-Phorades 1997," *Rep. Dep. Antiquities, Cyprus*, 247–68 (1998).

¹²A. B. Knapp, V. Kassianidou, and M. Donnell, "Excavations at Politiko-Phorades 1998," *Rep. Dep. Antiquities, Cyprus*, 125–46 (1999).

¹³E. Y. Litovsky and M. Shapiro, "Gas Pressure and Temperature Dependences of Thermal Conductivity of Porous Ceramic Materials: Part 1, Refractories and Ceramics with Porosity Below 30," *J. Am. Ceram. Soc.*, **75** [12] 3425–39 (1992).

¹⁴W. D. Kingery, H. K. Bowen, and D. R. Uhlmann, *Introduction to Ceramics*, 2nd edition, John Wiley & Sons, New York, 1976.

¹⁵J. C. Maxwell, *Treatise on Electricity and Magnetism*, Vol. 1. Oxford University Press, London, 1892.

¹⁶F. Cernuschi, S. Ahmaniemi, P. Vuoristo, and T. Mantyla, "Modelling of Thermal Conductivity of Porous Materials: Application to Thick Thermal Barrier Coatings," *J. Europ. Ceram. Soc.*, **24**, 2657–67 (2004).

¹⁷P. M. Day, M. Relaki, and E. W. Faber, "Pottery Making and Social Reproduction in the Bronze Age Mesara"; pp. 22–72 in *Pottery and Society: The Impact of Recent Studies in Minoan Pottery*, Edited by M. H. Weiner, J. L. Warner, J. Polonsky, and E. E. Hayes. Archaeological Institute of America, Boston, 2006.

¹⁸S.-H. Leigh and C. C. Berndt, "Quantitative Evaluation of Void Distributions within a Plasma-Sprayed Ceramic," *J. Am. Ceram. Soc.*, **82** [1] 17–21 (1999).

¹⁹K. Bakker, "Using the Finite Element Method to Compute the Influence of Complex Porosity and Inclusion Structures on the Thermal and Electrical Conductivity," *Int. J. Heat Mass Transfer*, **40** [15] 3503–11 (1997).

²⁰A. P. Roberts and E. J. Garboczi, "Elastic Properties of Model Porous Ceramics," *J. Am. Ceram. Soc.*, **83** [12] 3041–8 (2000).

²¹E. Y. Litovsky, M. Shapiro, and A. Shavit, "Gas Pressure and Temperature Dependences of Thermal Conductivity of Porous Ceramic Materials: Part 2. Refractories and Ceramics with Porosity Exceeding 30," *J. Am. Ceram. Soc.*, **79** [5] 1366–76 (1996).

²²A. Hein and V. Kilikoglou, "Finite Element Analysis (FEA) of Metallurgical Ceramics: Assessment of their Thermal Behaviour"; in *Aegean Metallurgy in the Bronze Age—Proceedings of the Symposium held in Rethymno, Crete, 19–21 November 2004*, Edited by I. Tzachili. Crete University Press, Heraklion, in press. □